Article

Discovery Medicine 2025; 37(202): 2702–2711
https://doi.org/10.24976/Discov.Med.202537202.226

Myricetin Mitigates Angiotensin II-Induced Atrial Fibrillation by Alleviating Endoplasmic Reticulum Stress-Induced Autophagy Through Inhibition of ESR1 Ubiquitination

Laisha Yan[1], Kechao Zhao[1], Lina Chen[1], Shunying Zhao[1,*]

[1]Department of Cardiac Surgery Intensive Care Unit, Ningbo Medical Center Lihuili Hospital, 315100 Ningbo, Zhejiang, China
*Correspondence: zhaoshunying222333@163.com (Shunying Zhao)
Submitted: 4 July 2025 Revised: 10 October 2025 Accepted: 20 October 2025 Published: 20 November 2025

Background: Atrial fibrillation (AF) is the most prevalent sustained arrhythmia, whose clinical management faces numerous challenges, including high recurrence rates and significant adverse effects associated with current therapies. Myricetin, a natural flavonoid compound, has shown unique therapeutic potential due to its multitarget cardioprotective properties and favorable safety profile. This study aimed to elucidate the specific molecular mechanisms through which myricetin mitigates AF.

Methods: Human atrial fibroblasts (hAFs) were transfected with or without short hairpin RNA (shRNA) targeting estrogen receptor 1 (ESR1) and subsequently exposed to various concentrations of myricetin and/or angiotensin II (Ang II). To examine the involvement of autophagy and oxidative stress, specific groups were treated with the autophagy inhibitor 3-methyladenine (3-MA) and the antioxidant N-acetyl cysteine (NAC). Then efficacy evaluation was performed employing 3-(4,5-Dimethylthiazol-2-yl)-2,5-diphenyltetrazolium bromide (MTT) assays for cell viability, quantitative reverse transcription polymerase chain reaction (qRT-PCR), western blot, flow cytometry, and co-immunoprecipitation (Co-IP) analyses.

Results: Myricetin effectively reversed Ang II-induced reductions in cell viability and increases in apoptosis ($p < 0.05$). It significantly stabilized ESR1 by attenuating reactive oxygen species (ROS)-dependent ubiquitination ($p < 0.001$), leading to marked decreases in endoplasmic reticulum (ER) stress markers (glucose-regulated protein 78 (GRP78), GRP94, and C/EBP homologous protein (CHOP)), as well as autophagy indicators (Beclin and microtubule-associated proteins 1A/1B light chain 3B (LC3II/LC3I)) ($p < 0.01$).

Conclusion: Myricetin emerges as a promising therapeutic candidate for AF management by reducing ESR1 ubiquitination and suppressing ER stress-related autophagy, thereby enhancing cellular resistance to stress-induced injury. These findings suggest that myricetin could be incorporated into existing AF therapeutic strategies to improve efficacy and safety outcomes.

Keywords: atrial fibrillation; estrogen receptor 1; myricetin; ubiquitination; endoplasmic reticulum stress-related autophagy

Introduction

Atrial fibrillation (AF) is the most prevalent form of sustained cardiac arrhythmia and contributes significantly to global morbidity and mortality [1,2]. The progression of AF is driven by complex atrial remodeling involving electrical, structural, and autonomic alterations [3,4]. Despite advances in pharmacological and interventional therapies, including antiarrhythmic drugs and catheter ablation, their overall effectiveness remains limited, particularly in elderly populations, due to modest efficacy, frequent recurrence, and considerable adverse effects [5,6]. Therefore, exploring alternative therapeutic strategies with improved safety and efficacy profiles is imperative.

Myricetin, a naturally occurring flavonoid found in numerous fruits and vegetables, has demonstrated notable cardioprotective properties [7,8]. It exhibits potent antioxidant activity and modulates multiple cellular signaling pathways relevant to cardiovascular homeostasis. Its antioxidant capacity contributes to mitigating oxidative stress and modulating cellular responses under pathological conditions, particularly in AF, where oxidative stress promotes atrial remodeling and arrhythmogenesis. Previous studies have reported that myricetin-rich compounds can attenuate cardiac fibrosis and improve cardiac function under stress conditions such as chronic hypoxia [9,10].

The link between oxidative stress and structural cardiac alterations highlights the importance of autophagy, a process for maintaining protein homeostasis [11]. Excessive activation of autophagy, often triggered by oxidative stress [12], may promote cardiac remodeling by degrading essential proteins and organelles [13,14]. Thus, by mitigating oxidative stress, myricetin may indirectly modulate autophagy pathways, which are vital for preserving cellular integrity and function under stress conditions. Con-

sistently, recent evidence indicates that autophagy-related genes serve as potential biomarkers and therapeutic targets in AF [15]. Autophagy is commonly induced by stimuli such as starvation, hypoxia, endoplasmic reticulum stress (ERS), and radiation [16]. ERS can activate the autophagy-lysosomal pathway, thereby playing a pivotal role in cardiac stress responses [17]. The intricate interplay between oxidative stress, autophagy, and AF underscores the potential of myricetin to modulate these interconnected pathways for therapeutic benefit.

To further elucidate the molecular mechanisms underlying the effects of myricetin in AF, we explored potential targets of myricetin using bioinformatics databases. Protein-protein interaction (PPI) analysis identified estrogen receptor 1 (ESR1) as a central node, and it was consequently selected for investigation. Recent research suggests that myricetin maintains stable interactions with ESR1 [18]. ESR1 participates in diverse cellular functions, including mitochondrial protection and modulation of ER stress [19,20]. Furthermore, ESR1 upregulates vascular endothelial growth factor A (VEGFA) [21], which has anti-fibrotic properties that may alleviate AF-associated structural remodeling. As AF progression is accompanied by elevated reactive oxygen species (ROS) levels [22], and the cardioprotective mechanism of myricetin involves ROS inhibition [23], the interplay between ESR1 and oxidative stress is central. Analysis of the Protein Lysine Modifications Database (PLMD) revealed the presence of ubiquitination modification sites on ESR1, suggesting that myricetin may enhance ESR1 expression by reducing ROS-dependent ubiquitination.

This study investigated how myricetin alleviates angiotensin II (Ang II)-induced AF by suppressing ROS-dependent ubiquitination of ESR1, thereby inhibiting ER stress-related autophagy. Elucidating this cellular mechanism will deepen our understanding of the therapeutic potential of myricetin in AF management.

Materials and Methods

Cell Culture and Treatment

Atrial fibrosis represents a key pathological feature in the onset and maintenance of AF [24]. Human atrial fibroblast cells (hAFs) (6320, ScienCell Research Laboratories, Carlsbad, CA, USA) were used to investigate the underlying mechanisms of AF. Cells were cultured in Dulbecco's Modified Eagle Medium (DMEM) (D6429, Sigma-Aldrich, St. Louis, MO, USA) supplemented with 10% fetal bovine serum (FBS) (9014-81-7, Sigma-Aldrich, St. Louis, MO, USA) and 1% penicillin-streptomycin (C0222, Beyotime, Shanghai, China) in a humidified incubator (37 °C, 5% CO_2). For experimental assays, hAFs were seeded in 96-well plates (for cell viability and apoptosis assays) or 6-well plates (for quantitative reverse transcription polymerase chain reaction (qRT-PCR) and western blotting) at appropriate densities. When cell confluence reached 70–80%, treatments were administered with 0/10/20/40/80/160 μM myricetin (M6760, Sigma-Aldrich, St. Louis, MO, USA) [23] and/or 1 μM Ang II [25] (4474-91-3, Sigma-Aldrich, St. Louis, MO, USA) according to the experimental design.

Specific treatment groups included exposure to N-acetyl cysteine (NAC, 5 mM, 3 h) [26] (616-91-1, Sigma-Aldrich, St. Louis, MO, USA) as a ROS scavenger in specific groups, and 3-methyladenine (3-MA, 1 mM, 3 h) [27] (5142-23-4, Sigma-Aldrich, St. Louis, MO, USA) as an autophagy inhibitor to explore the regulatory effects of myricetin and ESR1 on ER stress-related autophagy. The hAF cell line was authenticated by short tandem repeat (STR) profiling and tested negative for mycoplasma contamination.

Transfection of ESR1 Silencing

To investigate the functional role of ESR1 in hAFs, gene silencing was performed using short hairpin RNA (shRNA). ESR1-specific shRNA (shESR1) was cloned into the pLKO.1 vector (Yunzhou Biosciences, Guangzhou, China), targeting the sequence 5′-GCAGGATTGTTGTGGCTACTA-3′. hAFs were cultured in DMEM containing 10% FBS until 70–80% confluence. For transfection, pLKO.1-short hairpin RNA negative control (shNC) (5′-CCTAAGGTTAAGTCGCCCTCG-3′) and pLKO.1-shESR1 plasmids were diluted in Opti-MEM (31985070, Thermo Fisher Scientific, Waltham, MA, USA), mixed with transfection reagent (C0526, Beyotime, Shanghai, China), and incubated for 20 min at 37 °C to form complexes. The complexes were then co-incubated with hAFs for 48 h to achieve gene silencing. Transfection efficiency was assessed using qRT-PCR. The experimental grouping for ESR1 silencing assays was as follows: Ang II (1 μM Ang II); Ang II + Myr (1 μM Ang II + 40 μM myricetin); Ang II + Myr + shNC (shNC + 1 μM Ang II + 40 μM myricetin); Ang II + Myr + shESR1 (shESR1 + 1 μM Ang II + 40 μM myricetin); Ang II + Myr + shESR1 + 3-MA (shESR1 + 1 μM Ang II + 40 μM myricetin + 1 mM 3-MA).

qRT-PCR

Total RNA was extracted from hAFs in the following groups: Control (no treatment), 0 (1 μM Ang II), 10 (1 μM Ang II + 10 μM myricetin), 20 (1 μM Ang II + 20 μM myricetin), 40 (1 μM Ang II + 40 μM myricetin), Ang II, Ang II + Myr, Ang II + Myr + shNC, Ang II + Myr + shESR1, and Ang II + Myr + shESR1 + 3-MA using TRIzol reagent (A33250, Thermo Fisher Scientific, Waltham, MA, USA). cDNA was synthesized using the SuperScript™ IV First-Strand Synthesis System (18091050, Thermo Fisher Scientific, Waltham, MA, USA). Reaction conditions were as follows: 25 °C for 12 min, 37 °C for 2 h, and 90 °C for 10 min to inactivate reverse transcriptase. qRT-PCR

was performed with quantitative real-time polymerase chain reaction (qPCR) Mix (K0253, Thermo Fisher Scientific, Waltham, MA, USA) using an Applied Biosystems platform (7500, Applied Biosystems, Foster City, CA, USA). Each 40 µL reaction mixture contained 20 µL qPCR Mix, 2 µL primer (10 µM, Tsingke Biotechnology, Beijing, China), 4 µL cDNA, and 12 µL nuclease-free water. Primer sequences were as follows: *ESR1*: Forward (F): 5′-TCTGCCAAGGGAGACTAGCTACT-3′, Reverse (R): 5′-GGTACATTGGTTTGTAGCTGGAC-3′; glyceraldehyde 3-phosphate dehydrogenase (*GAPDH*): F: 5′-AAGGTGAAGGTCGGAGTCAA-3′, R: 5′-AATGAAGGGGTCATTGATGG-3′.

Thermal cycling parameters were: initial denaturation at 90 °C for 15 min, followed by 35 cycles of 90 °C for 15 s, 65 °C for 30 s, and 68 °C for 30 s. A melting curve analysis was subsequently conducted, and relative mRNA expression levels were calculated using the $2^{-\Delta\Delta Ct}$ method.

3-(4,5-Dimethylthiazol-2-yl)-2,5-Diphenyltetrazolium Bromide (MTT) Assay

Cell viability was assessed using the MTT assay. Briefly, hAFs from the Control, 0, 10, 20, 40, 80, 160; Ang II, Ang II + Myr, Ang II + Myr + shNC, Ang II + Myr + shESR1, and Ang II + Myr + shESR1 + 3-MA groups were incubated with 20 µL MTT solution (5 mg/mL) (M6494, Thermo Fisher Scientific, Waltham, MA, USA) for 4 h at 37 °C. The resulting formazan crystals were dissolved in 200 µL dimethyl sulfoxide (DMSO) (ST038, Beyotime, Shanghai, China), and absorbance was measured at 570 nm using a microplate reader (SpectraMax ABS Plus, Molecular Devices, San Jose, CA, USA). Following optical density (OD) measurements, the average OD value of each group was calculated to evaluate cell viability. The percentage of viable cells was determined using the following equation:

$$\text{Cell viability (\%)} = (OD_{Experimental} - OD_{Blank}) / (OD_{Control} - OD_{Blank}) \times 100$$

Flow Cytometry

hAFs were cultured and treated according to the following groupings: Control (no treatment), Myr (40 µM myricetin), Ang II (1 µM Ang II), Ang II + Myr (1 µM Ang II + 40 µM myricetin), Ang II, Ang II + Myr, Ang II + Myr + shNC, Ang II + Myr + shESR1, and Ang II + Myr + shESR1 + 3-MA. The Annexin fluorescein isothiocyanate (FITC) Cell Apoptosis Kit (640914, BioLegend, San Diego, CA, USA) was used to evaluate apoptosis. 24 h after treatment, cells were detached using trypsin-ethylene diamine tetraacetic acid (C0201, Beyotime, Shanghai, China) and neutralized with complete medium. Following centrifugation, the collected cells were washed with PBS, and the pellet was resuspended in 195 µL of 1× binding buffer. Cells were stained with 5 µL Annexin V-FITC and 10 µL propidium iodide (PI) for 15 min, at room temperature in the darkness, followed by the addition of 400 µL 1× binding buffer per sample. Apoptotic cells were analyzed using a NovoCyte Penteon flow cytometer (Agilent Technologies, Santa Clara, CA, USA). FITC and PI fluorescence were measured to identify early apoptotic cells (Annexin V-positive, PI-negative) and late apoptotic cells (positive for both markers).

Western Blot Analysis

Protein expression levels of glucose-regulated protein 78 (GRP78, 75 kDa), GRP94 (94 kDa), C/EBP homologous protein (CHOP, 31 kDa), Beclin (52 kDa), microtubule-associated proteins 1A/1B light chain 3B (LC3I, 14 kDa; LC3II, 16 kDa), ESR1 (66 kDa) and GAPDH (40 kDa, internal control) were analyzed by western blotting [28]. hAFs from Control, Myr, Ang II, Ang II + Myr; Ang II, Ang II + Myr, Ang II + Myr + shNC, Ang II + Myr + shESR1, and Ang II + Myr + shESR1 + 3-MA groups were lysed in radio immunoprecipitation assay (RIPA) buffer containing protease and phosphatase inhibitors (89900, Thermo Fisher Scientific, Waltham, MA, USA). Lysates were centrifuged (14,000 ×g, 20 min, 4 °C), and the supernatant containing total protein was collected. Protein concentrations were determined using the bicinchoninic acid (BCA) Protein Assay Kit (08W00021, MP Biomedicals, Irvine, CA, USA).

Equal amounts of protein were separated by sodium dodecyl sulfate-polyacrylamide gel electrophoresis (SDS-PAGE) and transferred onto polyvinylidene fluoride (PVDF) membranes (F619537-0001, Sangon Biotech, Shanghai, China). After blocking with 5% skim milk for 1 h, membranes were incubated overnight at 4 °C with primary antibodies (Abcam, Cambridge, UK): GRP78 (ab21685), GRP94 (ab238126), CHOP (ab11419), Beclin (ab207612), LC3 (ab192890), ESR1 (ab237995), and GAPDH (ab9485). Following three washes with tris buffered saline with Tween-20 (TBST), membranes were incubated with secondary antibodies: ab150113 (for CHOP/ESR1) and ab205718 for other targets (24 °C, 1 h). Protein bands were visualized using an enhanced chemiluminescence (ECL) system (Amersham Pharmacia, Piscataway, NJ, USA). Band intensities were quantified using ImageJ software (Version 1.53, National Institutes of Health, Bethesda, MD, USA) and normalized to GAPDH (loading control). Data were expressed as fold changes relative to the control group.

Co-Immunoprecipitation (Co-IP) Analysis

The ubiquitination status of ESR1 in hAFs from Control, Ang II, Ang II + Myr, and Ang II + Myr + NAC groups was analyzed using Co-IP. Total protein was extracted as described for the western blot assay. Lysates were incubated overnight with protein A/G magnetic beads (88804, Thermo Fisher Scientific, Waltham, MA, USA) conjugated to ESR1 antibodies (8644, Cell Signaling Technology, Danvers, MA, USA), while normal immunoglobulin G (IgG) (A7016, Beyotime, Shanghai, China) served as the negative

control. Beads were washed to remove unbound proteins and nonspecific contaminants, followed by elution of bound protein by heating. Eluates were subjected to SDS-PAGE and western blotting, and ubiquitination of ESR1 was detected using an anti-ubiquitin antibody (SPC-119B, Stress-Marq Biosciences Inc., Victoria, BC, Canada).

ROS Measurement

To assess oxidative stress in hAFs from the Control, Myr, Ang II, and Ang II + Myr groups, the dihydroethidium (DHE) Assay Kit (S0064S, Beyotime, Shanghai, China) was employed [29]. After treatment, cells were stained with DHE and incubated for 30 min at 37 °C in the dark to allow ROS to react with DHE. Antimycin A was used as a positive control (1 h). Following the removal of the staining solution and cell washing, fluorescence intensity was measured. A fluorescence microscope (BX53, Olympus Life Science, Tokyo, Japan) equipped with excitation and emission filters (480–520 nm and 570–600 nm, respectively) was employed to detect the oxidized form of DHE, reflecting intracellular ROS levels. ROS generation was quantified as follows:

Relative DHE fluorescence = fluorescence intensity of experimental group / fluorescence intensity of control group

Statistical Analysis

All data analyses were performed using GraphPad Prism 8.0 (GraphPad Software, San Diego, CA, USA). Multiple group comparisons were performed using one-way ANOVA followed by Tukey's post hoc test. The Shapiro-Wilk test was used to assess data normality, while the Brown-Forsythe test was used for homogeneity of variance. Statistical significance was set at $p < 0.05$. Results were presented as mean ± standard deviation (SD).

Results

Modulatory Effects of Myricetin on Cellular Viability and Stress Response in hAFs

The viability of hAFs remained comparable under treatment with 0, 10, 20, or 40 μM myricetin but was significantly reduced by 80 μM and 160 μM myricetin (Fig. 1A, $p < 0.01$). Therefore, concentrations of 0, 10, 20, and 40 μM were selected for further experiments. Ang II treatment markedly decreased hAF viability (Fig. 1B, $p < 0.001$). However, myricetin at 20/40 μM effectively reversed this reduction (Fig. 1B, $p < 0.05$), which corresponded with its regulatory effect on ESR1 expression. qRT-PCR analysis revealed that Ang II significantly downregulated *ESR1* mRNA expression, whereas myricetin treatment restored ESR1 levels (Fig. 1C, $p < 0.001$). Among the tested concentrations, 40 μM myricetin yielded the highest ESR1 expression and maximal cell viability; therefore, it was used in subsequent experiments.

Flow cytometry revealed that 40 μM myricetin had minimal effect on apoptosis in normal hAFs (Fig. 1D,E, $p > 0.05$), indicating its non-toxic profile at this concentration. However, myricetin significantly reduced apoptosis in Ang II-treated cells (Fig. 1D,E, $p < 0.001$), underscoring its protective role against Ang II-induced cellular injury. Western blot analysis further indicated that myricetin reduced the LC3II/LC3I ratio compared with the Control group in normal cells (Fig. 1F,K, $p < 0.001$). Expression levels of GRP78, GRP94, CHOP, Beclin, and LC3II/LC3I were significantly elevated in the Ang II group relative to the Control group (Fig. 1F–K, $p < 0.001$). Conversely, these protein levels were markedly decreased in the Ang II + Myr group compared with Ang II alone (Fig. 1F–K, $p < 0.001$), while they remained higher (except for CHOP) in the Ang II + Myr group compared with the Myr group (Fig. 1F–H,J,K, $p < 0.05$).

Impacts of Myricetin on Oxidative Stress and Protein Stability in hAFs

ROS levels, as indicated by DHE staining, were significantly decreased in hAFs treated with 40 μM myricetin (Fig. 2A,B, $p < 0.001$). In the presence of Ang II, myricetin treatment further reduced ROS levels (Fig. 2A,B, $p < 0.001$), highlighting its role in mitigating oxidative stress. Western blot analysis revealed upregulated ESR1 protein expression in myricetin-treated cells, and ESR1 levels were higher in the Ang II + Myr group compared with the Ang II group (Fig. 2C,D, $p < 0.001$), demonstrating that myricetin counteracts Ang II-induced ESR1 suppression.

Co-IP assays further demonstrated that ESR1 ubiquitination was elevated and ESR1 protein expression decreased in the Ang II group (Fig. 2E–G, $p < 0.05$), indicating that Ang II promotes ubiquitin-mediated degradation of ESR1. In contrast, the Ang II + Myr group displayed reduced ESR1 ubiquitination and increased ESR1 protein levels (Fig. 2E–G, $p < 0.001$), suggesting that myricetin prevents ESR1 degradation by inhibiting its ubiquitination. Moreover, NAC treatment further inhibited ESR1 ubiquitination (Fig. 2E–G, $p < 0.001$) and significantly increased ESR1 protein expression, implying that ROS-dependent ubiquitination of ESR1 contributes to its degradation. These findings suggest that myricetin alleviates Ang II-induced AF, at least in part, by suppressing ROS-mediated ESR1 ubiquitination and ER stress-related autophagy.

Effects of Myricetin and ESR1 on ER Stress-Related Autophagy

To understand the specific roles of ESR1 and autophagy in regulating cellular responses under stress, hAFs were treated with myricetin and Ang II in combination with ESR1 silencing and autophagy inhibition. qRT-PCR and western blot analyses unraveled significantly reduced ESR1 expression in the Ang II + Myr + shESR1 group compared with the Ang II + Myr + shNC group (Fig. 3A–D, $p < 0.05$), confirming successful transfection. This effect of shESR1 persisted despite autophagy inhibition, as ESR1 levels re-

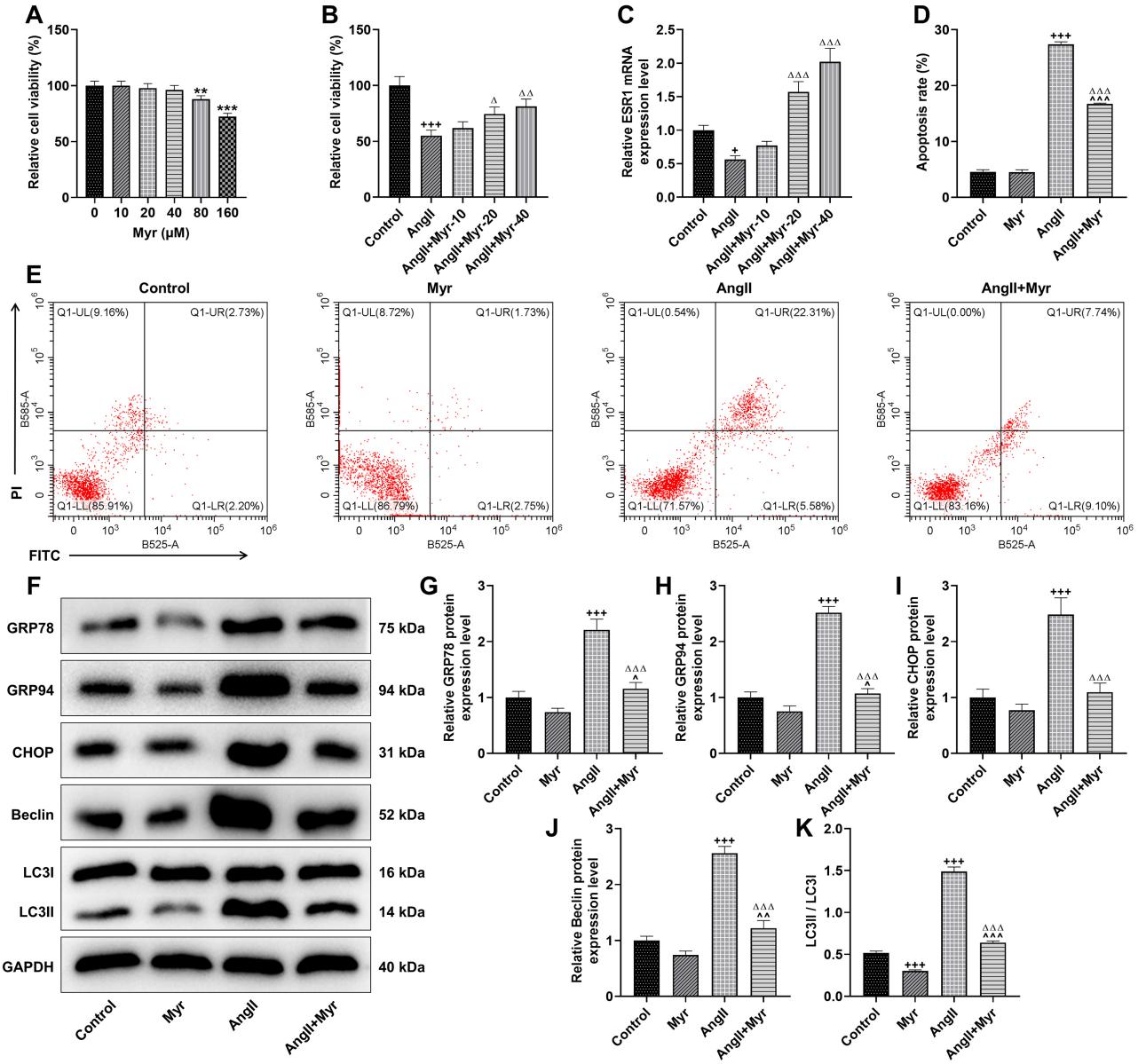

Fig. 1. Modulatory effects of myricetin on cellular viability and stress response in human atrial fibroblasts (hAFs). (A) Effects of 0, 10, 20, 40, 80, and 160 μM myricetin (Myr) on hAFs viability (3-(4,5-Dimethylthiazol-2-yl)-2,5-diphenyltetrazolium bromide (MTT)); (B) Effects of myricetin on angiotensin II (Ang II)-induced reduction in hAF viability (MTT assay); (C) Effects of Ang II and myricetin on estrogen receptor 1 (*ESR1*) expression (quantitative reverse transcription polymerase chain reaction (qRT-PCR)); (D) Apoptosis rates (quantitative analysis); (E) Cell apoptosis in each group (flow cytometry; numbers in plots indicate the percentage of apoptotic cells); (F) Protein expressions of glucose-regulated protein 78 (GRP78), GRP94, C/EBP homologous protein (CHOP), Beclin, and microtubule-associated proteins 1A/1B light chain 3B (LC3II/LC3I) (western blotting); (G–K) Quantitative analyses of GRP78, GRP94, CHOP, Beclin, and LC3II/LC3I expression levels. GAPDH served as the internal reference. ** vs. 0 μM Myr, ** $p < 0.01$, *** $p < 0.001$; $^{+}$ vs. Control, $^{+}$ $p < 0.05$, $^{+++}$ $p < 0.001$; $^{\wedge}$ vs. Myr, $^{\wedge}$ $p < 0.05$, $^{\wedge\wedge}$ $p < 0.01$, $^{\wedge\wedge\wedge}$ $p < 0.001$; $^{\Delta}$ vs. Ang II, $^{\Delta}$ $p < 0.05$, $^{\Delta\Delta}$ $p < 0.01$, $^{\Delta\Delta\Delta}$ $p < 0.001$. Data represent means ± SD from three independent experiments (n = 3). PI, propidium iodide; FITC, fluorescein isothiocyanate; GAPDH, glyceraldehyde 3-phosphate dehydrogenase.

mained unchanged between the Ang II + Myr + shESR1 and Ang II + Myr + shESR1 + 3-MA groups (Fig. 3B–D).

Cell viability was significantly lower in the Ang II + Myr + shESR1 group than in the Ang II + Myr + shNC group (Fig. 3E, $p < 0.001$), indicating that ESR1 silencing reduced cell viability. However, cell viability was notably enhanced in the Ang II + Myr + shESR1 + 3-MA group compared with the Ang II + Myr + shESR1 group (Fig. 3E, $p < 0.001$), demonstrating that autophagy inhibition can partially restore cell viability suppressed by

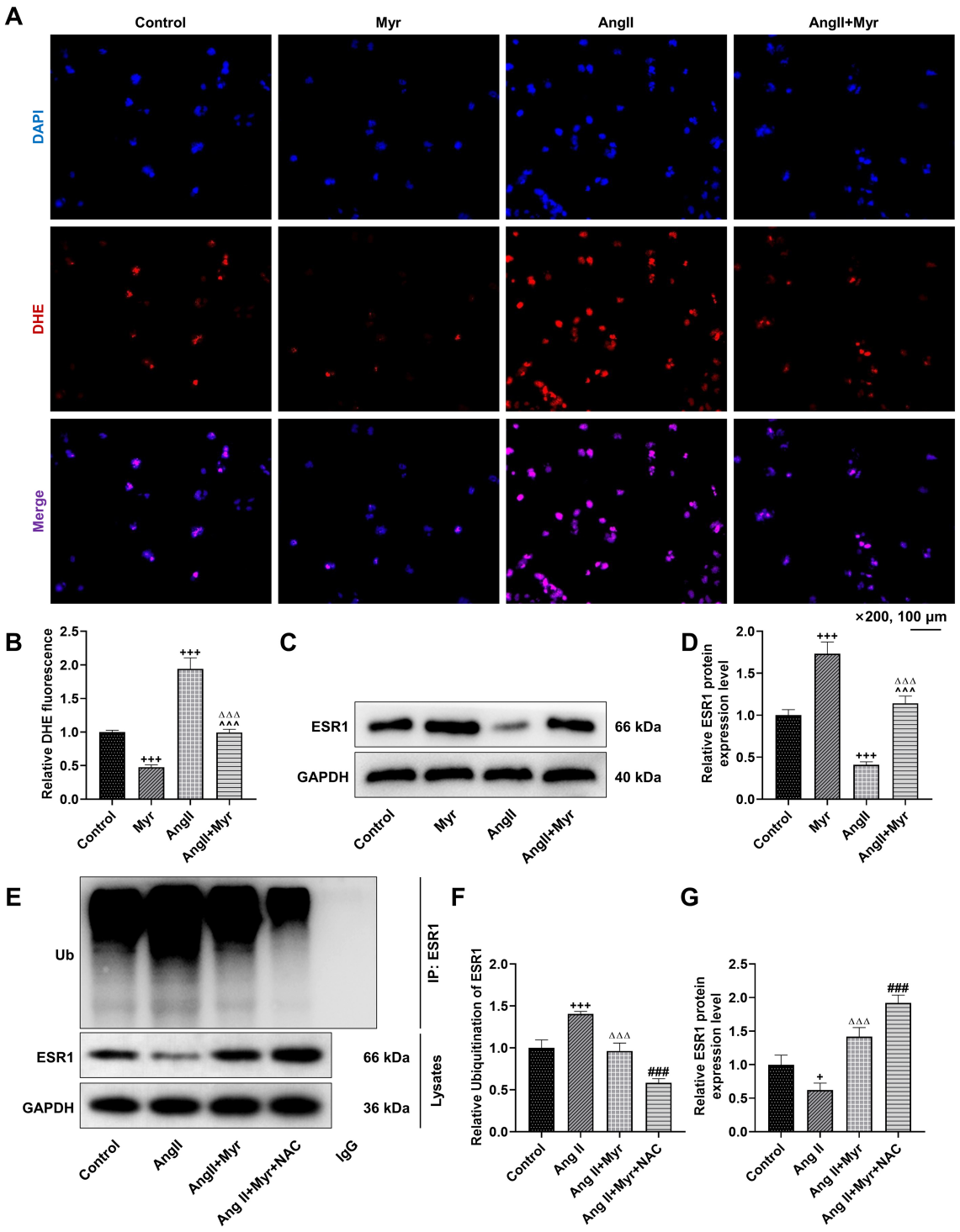

Fig. 2. Impacts of myricetin on oxidative stress and protein stability in hAFs. (A) Oxidative stress levels using dihydroethidium (DHE) Assay Kit. DHE (red) was employed to detect reactive oxygen species (ROS), where red fluorescence indicates the presence of ROS. DAPI (blue) stained nuclei, and merged images showed ROS-nuclei colocalization. Microscopy was performed at 200× magnification (scale bar = 100 μm); (B) Quantification of DHE fluorescence intensity; (C) ESR1 protein expression (western blotting; GAPDH as internal reference; (D) Quantitative analysis of ESR1 protein levels; (E–G) ESR1 ubiquitination analysis (co-immunoprecipitation, Co-IP; GAPDH as internal reference). $^{+}$ vs. Control, $^{+}$ $p < 0.05$, $^{+++}$ $p < 0.001$; $^{\Delta\Delta\Delta}$ vs. Ang II, $^{\Delta\Delta\Delta}$ $p < 0.001$; $^{\wedge\wedge\wedge}$ vs. Myr, $^{\wedge\wedge\wedge}$ $p < 0.001$; $^{\#\#\#}$ vs. Ang II + Myr, $^{\#\#\#}$ $p < 0.001$. Data represent means ± SD from three independent experiments (n = 3). IgG, immunoglobulin G; Ub, ubiquitin; IP, immunoprecipitation; DAPI, 4′6-diamidino-2-phenylindole; NAC, N-acetyl cysteine.

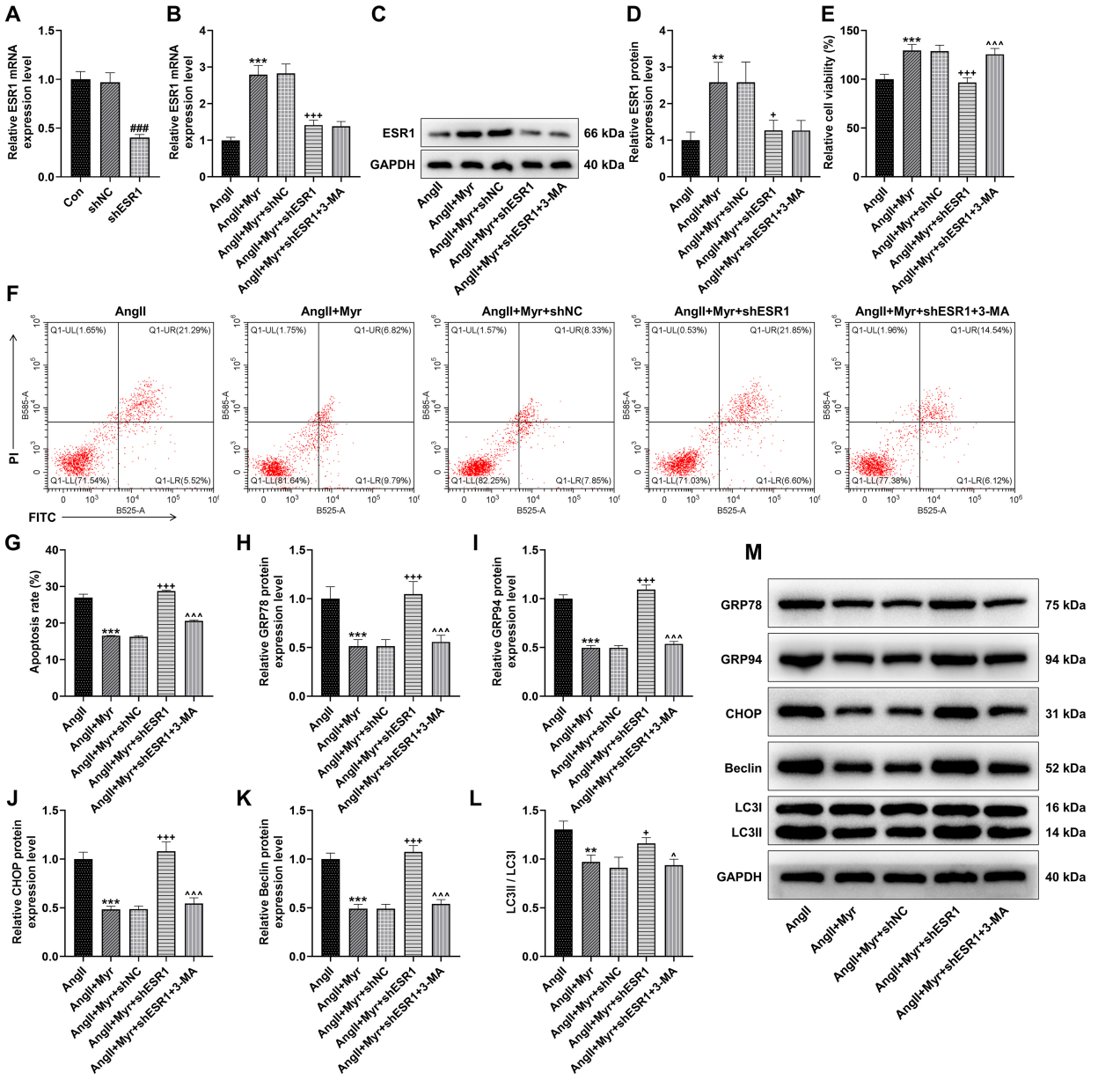

Fig. 3. Effects of myricetin and ESR1 on endoplasmic reticulum (ER) stress-related autophagy. (A) *ESR1* transfection efficiency (qRT-PCR); (B) *ESR1* mRNA expression (qRT-PCR; *GAPDH* as internal reference); (C) ESR1 protein expression (western blotting; GAPDH as internal reference); (D) Quantitative analysis of ESR1 protein levels; (E) Cell viability (MTT assay); (F) Apoptotic cell population in each group (flow cytometry; numbers in the plots indicate the percentage of apoptotic cells; (G) Quantitative analysis of apoptosis rates; (H–L) Quantitative analysis of GRP78, GRP94, CHOP, Beclin, and LC3II/LC3I proteins expression; (M) GRP78, GRP94, CHOP, Beclin, and LC3II/LC3I protein expression (western blotting, GAPDH as the internal reference). $^{###}$ vs. shNC, $^{###}$ $p < 0.001$; ** vs. Ang II, ** $p < 0.01$, *** $p < 0.001$; $^{+}$ vs. Ang II + Myr + shNC, $^{+}$ $p < 0.05$, $^{+++}$ $p < 0.001$; $^{\wedge}$ vs. Ang II + Myr + shESR1, $^{\wedge}$ $p < 0.05$, $^{\wedge\wedge\wedge}$ $p < 0.001$. Data represent means ± SD from three independent experiments (n = 3). 3-MA, 3-methyladenine; shESR1, ESR1-specific shRNA; shNC, short hairpin RNA negative control.

ESR1 silencing. Consistent with these findings, flow cytometry revealed a significant increase in apoptosis in the Ang II + Myr + shESR1 group compared with the Ang II + Myr + shNC group (Fig. 3F,G, $p < 0.001$), suggesting that ESR1 silencing promotes apoptosis. The apoptosis rate was markedly reduced in the Ang II + Myr + shESR1 + 3-MA group relative to the Ang II + Myr + shESR1 group (Fig. 3F,G, $p < 0.001$), indicating that autophagy inhibition counteracts ESR1 silencing-induced apoptosis.

Western blot analysis further elucidated the underlying molecular mechanisms involved, where GRP78, GRP94, CHOP, Beclin, and LC3II/LC3I ratio were signif-

icantly higher in the Ang II + Myr + shESR1 group than in the Ang II + Myr + shNC group (Fig. 3H–M, $p < 0.05$), suggesting that ESR1 silencing reactivates ER stress and autophagy. Conversely, these protein levels were markedly reduced in the Ang II + Myr + shESR1 + 3-MA group compared with the Ang II + Myr + shESR1 group (Fig. 3H–M, $p < 0.05$), demonstrating that autophagy inhibition alleviates ESR1 silencing-induced ER stress and autophagy.

Overall, these findings demonstrate that myricetin markedly enhances ESR1 expression, improves cell viability, and suppresses apoptosis and autophagy under Ang II-induced stress conditions. Nevertheless, ESR1 silencing attenuates these protective effects of myricetin, emphasizing the pivotal role of ESR1 in mediating the protective effects of myricetin against cellular stress. Notably, application of autophagy inhibitors effectively mitigated the adverse outcomes associated with ESR1 silencing, such as reduced cell viability and increased apoptosis and ER stress, without altering ESR1 expression.

Discussion

Although current strategies for managing AF, including pharmacological interventions and catheter ablation, provide valuable treatment options, they often fail to prevent recurrence and carry considerable side effects, particularly among elderly patients [5,6,30]. This highlights the urgent need for novel, effective, and better-tolerated therapeutic approaches. Our study demonstrated that myricetin enhances atrial fibroblast activation by regulating ESR1 ubiquitination and attenuating ERS-associated autophagy. These findings identify a potential novel therapeutic target for AF management, particularly addressing clinical challenges such as high recurrence rates and suboptimal treatment tolerance in elderly patients.

One of the key mechanisms of myricetin is its ability to reduce the ubiquitination of ESR1, a key regulatory protein involved in numerous cellular processes, including stress response and mitochondrial homeostasis [19]. Our data revealed that myricetin significantly reduced ESR1 ubiquitination, thereby preserving ESR1 expression, while ESR1 silencing induced ER stress and autophagy. Consistent with previous research, ESR1 downregulation has been shown to cause abnormal activation of autophagy [31], suggesting that ESR1 plays a pivotal role in ER stress and autophagy. Furthermore, ER stress-related genes (*GRP78*, *GRP94*, and *CHOP*) are highly expressed in AF [32], highlighting the critical role of ER stress in disease progression. The involvement of these stress markers in AF supports the rationale for therapeutically targeting these pathways. Similarly, our findings demonstrated that myricetin suppressed the expression of GRP78, GRP94, CHOP, Beclin, and LC3II/LC3I in Ang II-induced cells.

Moreover, the potential of myricetin to modulate ER stress-related autophagy warrants deeper investigation, as autophagy exerts a dual role, either promoting survival or inducing death under different cellular conditions [12]. The precise mechanisms by which myricetin regulates this balance, particularly its effects on fibroblast autophagy in AF, remain incompletely defined. Future research should focus on elucidating the bidirectional regulatory effects of myricetin on autophagy under diverse pathological conditions to better clarify its therapeutic window and associated risks. Such studies will not only optimize the application of myricetin in AF treatment but also provide theoretical foundations for developing novel therapeutics that target cellular stress resistance pathways.

Notably, several limitations of this study should be acknowledged. The *in vitro* design limits direct clinical translation. Although hAFs are a relevant model, they cannot fully replicate the complex *in vivo* environment of atrial tissue in AF patients, especially in terms of interactions with other cell types and systemic immune components. Future studies incorporating animal models will be essential to determine whether these findings hold true *in vivo* and to investigate whether ESR1 exhibits tissue-specific expression alterations during AF pathogenesis. Moreover, the myricetin concentrations used in this study, although effective *in vitro*, require thorough *in vivo* validation to confirm their safety and therapeutic efficacy in human subjects.

Conclusion

In conclusion, our study confirms that myricetin modulates key molecular pathways involved in the activation of atrial fibroblasts, primarily by regulating ESR1, reducing ER stress, and inhibiting autophagy. These findings suggest a novel therapeutic approach to AF management that may complement existing treatment modalities, offering a strategy that combines efficacy with a potentially improved safety profile. Future investigations should aim to elucidate the detailed mechanisms by which myricetin influences protein ubiquitination and autophagy in atrial cells, while exploring its broader therapeutic potential in diseases characterized by protein misfolding and cellular stress, such as Alzheimer's disease and diabetes.

Availability of Data and Materials

The datasets used and analyzed during the current study are available from the corresponding author upon reasonable request.

Author Contributions

LY designed the research study; LY, KZ, LC and SZ performed the research; LY, KZ and LC collected and analyzed the data. LY and SZ have been involved in drafting the manuscript and all authors have been involved in revising it critically for important intellectual content. All authors give final approval of the version to be published.

All authors have participated sufficiently in the work to take public responsibility for appropriate portions of the content and agreed to be accountable for all aspects of the work in ensuring that questions related to its accuracy or integrity.

Ethics Approval and Consent to Participate

Not applicable.

Acknowledgment

Not applicable.

Funding

This work was supported by the Zhejiang Province Traditional Chinese Medicine Science and Technology Plan Project [grant number: 2024ZL939].

Conflict of Interest

The authors declare no conflict of interest.

References

[1] Smith EE, Yaghi S, Sposato LA, Fisher M. Atrial Fibrillation Detection and Load: Knowledge Gaps Related to Stroke Prevention. Stroke. 2024; 55: 205–213. https://doi.org/10.1161/STROKEAHA.123.043665.

[2] Welker CC, Ramakrishna H. Postoperative Atrial Fibrillation: Guidelines Revisited. Journal of Cardiothoracic and Vascular Anesthesia. 2023; 37: 2413–2415. https://doi.org/10.1053/j.jvca.2023.07.040.

[3] Essa H, Hill AM, Lip GYH. Atrial Fibrillation and Stroke. Cardiac Electrophysiology Clinics. 2021; 13: 243–255. https://doi.org/10.1016/j.ccep.2020.11.003.

[4] Jame S, Barnes G. Stroke and thromboembolism prevention in atrial fibrillation. Heart (British Cardiac Society). 2020; 106: 10–17. https://doi.org/10.1136/heartjnl-2019-314898.

[5] Saljic A, Heijman J, Dobrev D. Emerging Antiarrhythmic Drugs for Atrial Fibrillation. International Journal of Molecular Sciences. 2022; 23: 4096. https://doi.org/10.3390/ijms23084096.

[6] Turagam MK, Musikantow D, Whang W, Koruth JS, Miller MA, Langan MN, *et al*. Assessment of Catheter Ablation or Antiarrhythmic Drugs for First-line Therapy of Atrial Fibrillation: A Meta-analysis of Randomized Clinical Trials. JAMA Cardiology. 2021; 6: 697–705. https://doi.org/10.1001/jamacardio.2021.0852.

[7] Liu J, Mamun Bhuyan AA, Ma K, Zhu X, Zhou K, Lang F. Myricetin-induced suicidal erythrocyte death. Molecular Biology Reports. 2023; 50: 4253–4260. https://doi.org/10.1007/s11033-023-08350-3.

[8] Song X, Tan L, Wang M, Ren C, Guo C, Yang B, *et al*. Myricetin: A review of the most recent research. Biomedicine & Pharmacotherapy. 2021; 134: 111017. https://doi.org/10.1016/j.biopha.2020.111017.

[9] Dang Z, Su S, Jin G, Nan X, Ma L, Li Z, *et al*. Tsantan Sumtang attenuated chronic hypoxia-induced right ventricular structure remodeling and fibrosis by equilibrating local ACE-AngII-AT1R/ACE2-Ang1-7-Mas axis in rat. Journal of Ethnopharmacology. 2020; 250: 112470. https://doi.org/10.1016/j.jep.2019.112470.

[10] Angelone T, Pasqua T, Di Majo D, Quintieri AM, Filice E, Amodio N, *et al*. Distinct signalling mechanisms are involved in the dissimilar myocardial and coronary effects elicited by quercetin and myricetin, two red wine flavonols. Nutrition, Metabolism, and Cardiovascular Diseases: NMCD. 2011; 21: 362–371. https://doi.org/10.1016/j.numecd.2009.10.011.

[11] Kroemer G, Mariño G, Levine B. Autophagy and the integrated stress response. Molecular Cell. 2010; 40: 280–293. https://doi.org/10.1016/j.molcel.2010.09.023.

[12] Wiersma M, Meijering RAM, Qi XY, Zhang D, Liu T, Hoogstra-Berends F, *et al*. Endoplasmic Reticulum Stress Is Associated With Autophagy and Cardiomyocyte Remodeling in Experimental and Human Atrial Fibrillation. Journal of the American Heart Association. 2017; 6: e006458. https://doi.org/10.1161/JAHA.117.006458.

[13] Zhang D, Wu CT, Qi X, Meijering RAM, Hoogstra-Berends F, Tadevosyan A, *et al*. Activation of histone deacetylase-6 induces contractile dysfunction through derailment of α-tubulin proteostasis in experimental and human atrial fibrillation. Circulation. 2014; 129: 346–358. https://doi.org/10.1161/CIRCULATIONAHA.113.005300.

[14] Brundel BJJM, Ausma J, van Gelder IC, Van der Want JJL, van Gilst WH, Crijns HJGM, *et al*. Activation of proteolysis by calpains and structural changes in human paroxysmal and persistent atrial fibrillation. Cardiovascular Research. 2002; 54: 380–389. https://doi.org/10.1016/s0008-6363(02)00289-4.

[15] Zhou J, Dong Y, Cai X, Yang H, Guo T. Identification and Validation of Autophagy-Related Genes as Potential Biomarkers and Therapeutic Targets in Atrial Fibrillation. International Journal of General Medicine. 2021; 14: 7783–7796. https://doi.org/10.2147/IJGM.S337855.

[16] Kundu M, Thompson CB. Autophagy: basic principles and relevance to disease. Annual Review of Pathology. 2008; 3: 427–455. https://doi.org/10.1146/annurev.pathmechdis.2.010506.091842.

[17] Kouroku Y, Fujita E, Tanida I, Ueno T, Isoai A, Kumagai H, *et al*. ER stress (PERK/eIF2alpha phosphorylation) mediates the polyglutamine-induced LC3 conversion, an essential step for autophagy formation. Cell Death and Differentiation. 2007; 14: 230–239. https://doi.org/10.1038/sj.cdd.4401984.

[18] Chowdhury MR, Karamveer K, Tiwary BK, Nampoothiri NK, Erva RR, Deepa VS. Integrated systems pharmacology, molecular docking, and MD simulations investigation elucidating the therapeutic mechanisms of BHD in Alzheimer's disease treatment. Metabolic Brain Disease. 2024; 40: 8. https://doi.org/10.1007/s11011-024-01460-2.

[19] Zhou Z, Ribas V, Rajbhandari P, Drew BG, Moore TM, Fluitt AH, *et al*. Estrogen receptor α protects pancreatic β-cells from apoptosis by preserving mitochondrial function and suppressing endoplasmic reticulum stress. The Journal of Biological Chemistry. 2018; 293: 4735–4751. https://doi.org/10.1074/jbc.M117.805069.

[20] Andruska ND, Zheng X, Yang X, Mao C, Cherian MM, Mahapatra L, *et al*. Estrogen receptor α inhibitor activates the unfolded protein response, blocks protein synthesis, and induces tumor regression. Proceedings of the National Academy of Sciences of the United States of America. 2015; 112: 4737–4742. https://doi.org/10.1073/pnas.1403685112.

[21] Fatima LA, Campello RS, Santos RDS, Freitas HS, Frank AP, Machado UF, *et al*. Estrogen receptor 1 (ESR1) regulates VEGFA in adipose tissue. Scientific Reports. 2017; 7: 16716. https://doi.org/10.1038/s41598-017-16686-7.

[22] Avula UMR, Dridi H, Chen BX, Yuan Q, Katchman AN, Reiken SR, *et al*. Attenuating persistent sodium current-induced atrial myopathy and fibrillation by preventing mitochondrial oxidative stress. JCI Insight. 2021; 6: e147371. https://doi.org/10.1172/jci.insight.147371.

[23] Chen S, Fan B. Myricetin protects cardiomyocytes from LPS-induced injury. Herz. 2018; 43: 265–274. https://doi.org/10.1007/s00059-017-4556-3.

[24] Gao XY, Lai YY, Luo XS, Peng DW, Li QQ, Zhou HS, *et al*. Acetyltransferase p300 regulates atrial fibroblast senescence and age-related atrial fibrosis through p53/Smad3 axis. Aging Cell. 2023; 22: e13743. https://doi.org/10.1111/acel.13743.

[25] Zhou Y, Xie Y, Li T, Zhang P, Chen T, Fan Z, *et al*. P21 activated kinase 1 mediates angiotensin II induced differentiation of human atrial fibroblasts via the JNK/c Jun pathway. Molecular Medicine Reports. 2021; 23: 207. https://doi.org/10.3892/mmr.2021.11846.

[26] Oh JM, Kim E, Chun S. Ginsenoside Compound K Induces Ros-Mediated Apoptosis and Autophagic Inhibition in Human Neuroblastoma Cells In Vitro and In Vivo. International Journal of Molecular Sciences. 2019; 20: 4279. https://doi.org/10.3390/ijms20174279.

[27] Kim KY, Yun UJ, Yeom SH, Kim SC, Lee HJ, Ahn SC, *et al*. Inhibition of Autophagy Promotes Hemistepsin A-Induced Apoptosis via Reactive Oxygen Species-Mediated AMPK-Dependent Signaling in Human Prostate Cancer Cells. Biomolecules. 2021; 11: 1806. https://doi.org/10.3390/biom11121806.

[28] Tian Q, Liu J, Chen Q, Zhang M. Andrographolide contributes to the attenuation of cardiac hypertrophy by suppressing endoplasmic reticulum stress. Pharmaceutical Biology. 2023; 61: 61–68. https://doi.org/10.1080/13880209.2022.2157021.

[29] Cheng Z, Zhang M, Hu J, Lin J, Feng X, Wang S, *et al*. Cardiac-specific Mst1 deficiency inhibits ROS-mediated JNK signalling to alleviate Ang II-induced cardiomyocyte apoptosis. Journal of Cellular and Molecular Medicine. 2019; 23: 543–555. https://doi.org/10.1111/jcmm.13958.

[30] Kirchhof P, Camm AJ, Goette A, Brandes A, Eckardt L, Elvan A, *et al*. Early Rhythm-Control Therapy in Patients with Atrial Fibrillation. The New England Journal of Medicine. 2020; 383: 1305–1316. https://doi.org/10.1056/NEJMoa2019422.

[31] Cook KL, Clarke PAG, Parmar J, Hu R, Schwartz-Roberts JL, Abu-Asab M, *et al*. Knockdown of estrogen receptor-α induces autophagy and inhibits antiestrogen-mediated unfolded protein response activation, promoting ROS-induced breast cancer cell death. FASEB Journal: Official Publication of the Federation of American Societies for Experimental Biology. 2014; 28: 3891–3905. https://doi.org/10.1096/fj.13-247353.

[32] Wang Y, Wang YL, Huang X, Yang Y, Zhao YJ, Wei CX, *et al*. Ibutilide protects against cardiomyocytes injury via inhibiting endoplasmic reticulum and mitochondrial stress pathways. Heart and Vessels. 2017; 32: 208–215. https://doi.org/10.1007/s00380-016-0891-1.